



HAL
open science

Template estimation form unlabeled point set data and surfaces for Computational Anatomy

Joan Alexis Glaunès, Sarang Joshi

► **To cite this version:**

Joan Alexis Glaunès, Sarang Joshi. Template estimation form unlabeled point set data and surfaces for Computational Anatomy. 1st MICCAI Workshop on Mathematical Foundations of Computational Anatomy: Geometrical, Statistical and Registration Methods for Modeling Biological Shape Variability, Oct 2006, Copenhagen, Denmark. hal-00263576

HAL Id: hal-00263576

<https://hal.science/hal-00263576v1>

Submitted on 12 Mar 2008

HAL is a multi-disciplinary open access archive for the deposit and dissemination of scientific research documents, whether they are published or not. The documents may come from teaching and research institutions in France or abroad, or from public or private research centers.

L'archive ouverte pluridisciplinaire **HAL**, est destinée au dépôt et à la diffusion de documents scientifiques de niveau recherche, publiés ou non, émanant des établissements d'enseignement et de recherche français ou étrangers, des laboratoires publics ou privés.

Template estimation form unlabeled point set data and surfaces for Computational Anatomy

Joan Glaunès¹ and Sarang Joshi²

¹ Center for Imaging Science, Johns Hopkins University, joan@cis.jhu.edu

² SCI, University of Utah, scjoshi@gmail.com

Abstract. A central notion in Computational Anatomy is the generation of registration maps, mapping a large set of anatomical data to a common coordinate system to study intra-population variability and inter-population differences. In previous work [1, 2] methods for estimating the common coordinate system or the template given a collection imaging data were presented based on the notion of Fréchet mean estimation using a metric on the space of diffeomorphisms. In this paper we extend the methodology to the estimation of a template given a collection of unlabeled point sets and surfaces. Using a representation of points and surfaces as currents a Reproducing Kernel Hilbert Space (RKHS) norm is induced on the space of Borel measures. Using this norm and a metric on the space of diffeomorphisms the template estimation problem is posed as a minimum mean squared error estimation problem. An efficient alternating conjugate gradient decent algorithm is derived and results exemplifying the methodology are presented.

1 Introduction

A major focus of computational anatomy has been the development of image mapping algorithms [3] that can map and transform a single brain atlas on to a population. Most digital brain atlases currently being used in computational anatomy are based on a single subjects anatomy. Although these atlases provide a standard coordinate system, and form the template in deformable template setting, they are limited because a single anatomy cannot faithfully represent the complex structural variability evident in a population.

Construction of atlases is a key procedure in population based medical image analysis. In the paradigm of computational anatomy the atlas serves as a deformable template[4]. The deformable template can project detailed atlas data such as structural, biochemical, functional as well as vascular information on to the individual or an entire population of brain images. The transformations encode the variability of the population under study. Statistical analysis of the transformations can be used to characterize different populations [5]. For a detailed review of deformable atlas mapping and the general framework for computational anatomy see [3].

1.1 Unbiased Large Deformation Atlas Estimation via minimum mean squared error estimation.

For representations in which the underlying geometry is parameterized as a Euclidean vector space, training data can be represented as a set of vectors x_1, \dots, x_N in a vector space V . In a vector space, with addition and scalar multiplication well defined, an average representation of the training set can be computed as the linear average $\mu = \frac{1}{N} \sum_i^N x_i$. When studying statistical geometric properties of anatomy, the transformations representing the variability of a population are parameterized via diffeomorphic transformations of the ambient space. In the group of diffeomorphisms, the addition of two diffeomorphisms is not generally a diffeomorphism and, hence, a template based on linear averaging of transformations is not well defined. Fréchet [6] extended the notation of averaging to general metric spaces via minimum mean squared error estimation. For a general metric space M , with a distance $d : M \times M \rightarrow R$, the intrinsic mean for a collection of data points $x_i \in M$ can be defined as the minimizer of the sum-of-squared distances to each of the data points. That is

$$\mu = \arg \min_x \frac{1}{N} \sum_i^N d(x, x_i)^2.$$

This approach, combined with the mathematical metric theory of diffeomorphisms developed in [7, 8], represents the core of the atlas estimation methodology. This approach has been applied previously to a sets of images, and can be stated as the following estimation problem. Given a metric, $D : S \times S \rightarrow R$ on a group of transformations, along with an image dissimilarity metric $E(I1, I2)$, we wish to find the image \hat{I} such that

$$\{\hat{\varphi}_i, \hat{I}\} = \arg \min_{\varphi_i, I} \frac{1}{N} \sum_i^N E(I_i \circ \varphi_i, I)^2 + D(e, \varphi_i)^2$$

where e is the identity transformation.

In this paper we follow the same basic paradigm for unlabeled point sets and surfaces. The paper is organized as follows: In section 2, following [9, ?], geometric measure theory is used to define dissimilarity metrics for unlabeled point sets and surfaces. For completeness in section 4 the metric on the space of diffeomorphisms is reviewed. In section 5 the template estimation problem given a collection of unlabeled point sets and surfaces is formulated. Finally in sections ?? 7 implementation details and results are presented.

2 Hilbert norms for dissimilarity metric for point set and surface data

2.1 Dissimilarity metric for unlabeled point sets and surface data

We follow the novel framework proposed in [9] for measuring dissimilarities between unlabeled point sets. Given a set of unlabeled landmark points $\{x_p\}_{p=1}^n$ in

\mathbb{R}^d , a vector space structure is induced on the space of all such unlabeled point sets by modeling them as a weighted sum of Dirac measures centered at each of the points that is: $\sum_{p=1}^n a_p \delta_{x_p}$. The weights $a_p \in \mathbb{R}$, such that $\sum_p a_p = 1$, are user-defined and capture the relative confidence associated with each landmark (without such information, one should simply set $a_p = \frac{1}{n}$ for each index p). The space of Dirac measures forms a vector space where point sets can be added and subtracted. A Dissimilarity metric is induced by a Reproducing Kernel Hilbert norm based on a user-defined kernel $K : \mathbb{R}^d \times \mathbb{R}^d \rightarrow \mathbb{R}$. The scalar product of two Dirac measures δ_x, δ_y is defined by the rule $\langle \delta_x, \delta_y \rangle_K = K(x, y)$, which leads to the following expression for the norm of the sum of Diracs:

$$\left\| \sum_{p=1}^n a_p \delta_{x_p} \right\|_K^2 = \sum_{p=1}^n \sum_{p'=1}^n a_p a_{p'} K(x_p, x_{p'}). \quad (1)$$

Dissimilarity between two points sets is given by the norm of the difference of the corresponding sums of Diracs:

$$\begin{aligned} \left\| \sum_{p=1}^n a_p \delta_{x_p} - \sum_{q=1}^m b_q \delta_{y_q} \right\|_K^2 &= \sum_{p=1}^n \sum_{p'=1}^n a_p a_{p'} K(x_p, x_{p'}) \\ &\quad - 2 \sum_{p=1}^n \sum_{q=1}^m a_p b_q K(x_p, y_q) + \sum_{q=1}^m \sum_{q'=1}^m b_q b_{q'} K(y_q, y_{q'}). \end{aligned} \quad (2)$$

These formulas arise naturally as the expression of the dual norm of the functional Hilbert space corresponding to the reproducing kernel K . We refer to [9] for all the mathematical details. In this setting, this dual norm is also defined, by mathematical completion with respect to the norm defined by Eqn. 1, for a larger class which include all signed Borel measures of \mathbb{R}^d . The K -norm of a measure μ is given by

$$\|\mu\|_K^2 = \iint K(x, y) d\mu(x) d\mu(y). \quad (3)$$

The action of a deformation map $\varphi : \mathbb{R}^d \rightarrow \mathbb{R}^d$ on a Borel measure μ satisfies $\varphi\mu(A) = \mu(\varphi^{-1}(A))$ for any subset $A \subset \mathbb{R}^d$. When μ is a sum of Dirac masses, it consists in moving all positions of points by φ , leaving the weights unchanged: $\varphi\left(\sum_{p=1}^n a_p \delta_{x_p}\right) = \sum_{p=1}^n a_p \delta_{\varphi(x_p)}$.

3 Hilbert norms for dissimilarity metric between surfaces

In [10], an extension of the above described method has been proposed to measure dissimilarities between oriented surfaces embedded in \mathbb{R}^3 . We recall its main point here. A convenient mathematical model of oriented m -dimensional submanifolds in \mathbb{R}^d with $m < d$, is the concept of "current", which comes from Geometric Measure Theory [11, 12]. Currents are generalizations of Schwartz distributions, where smooth test functions are replaced by smooth m -differential forms

in \mathbb{R}^d , i.e. smooth maps ω that associate to each point $x \in \mathbb{R}^d$ a skew-symmetric m -multilinear form, or m -covector, $\omega(x)$. Hence currents can be viewed as generalized m -forms, or as linear functionals acting on m -forms. The current associated to an oriented m -submanifold S is the linear functional $[S]$ defined by $[S](\omega) = \int_S \omega$. When S is an oriented surface in \mathbb{R}^3 , $[S]$ is nothing but the vector valued Borel measure corresponding to the collection of unit-normal vectors to S , distributed with density equal to the element of surface area ds and can be written as $\eta(y)ds(y)$, where $\eta(y)$ is the normal and $ds(y)$ is the surface measure at point $y \in S$.

In this setting, similarly to what was described above for scalar measures, one can introduce a matrix-valued kernel $K(x, y)$ and define the K -norm of $[S]$ by

$$\| [S] \|_K^2 = \int_S \int_S \eta(y)^* K(x, y) \eta(x) ds(x) ds(y). \quad (4)$$

In practice we use kernels of the type $k(x, y)I$ where I is a 3×3 identity matrix and $k(x, y)$ a scalar kernel of the Gaussian or the Cauchy type. Then the integrand in Eqn. 4 becomes $K(x, y) \langle \eta(x), \eta(y) \rangle$. When S is a triangular mesh, a good approximation of this formula can be computed by replacing $[S]$ by a sum of vector-valued Dirac masses:

$$\left\| \sum_{f=1}^{nf} \eta(f) \delta_{c(f)} \right\|_K^2 = \sum_{f=1}^{nf} \sum_{f'=1}^{nf} \eta(f')^* K(c(f), c(f')) \eta(f), \quad (5)$$

where nf is the number of faces of the triangulation, and for any face f with vertices x, y, z , $c(f)$ is its center and $\eta(f)$ its non-normalized normal vector with the length capturing the area of each triangular patch:

$$c(f) = \frac{1}{3}(x + y + z), \quad \eta(f) = \frac{1}{2}(y - x) \times (z - x). \quad (6)$$

The sum $\sum_{f=1}^{nf} \eta(f) \delta_{c(f)}$ does not correspond to a surface, but it is close to $[S]$ in the space of currents.

One can mathematically define an action of deformation maps $\varphi : \mathbb{R}^3 \rightarrow \mathbb{R}^3$ on currents, called push-forward, which is consistent to the intuitive action on subset of \mathbb{R}^3 . This means that for a surface S , the push-forward $\varphi[S]$ is exactly the current associated to the deformed surface: $\varphi[S] = [\varphi(S)]$. For a sum of Diracs, the push-forward action becomes:

$$\varphi \left(\sum_{f=1}^{nf} \eta(f) \delta_{c(f)} \right) = \sum_{f=1}^{nf} |d\varphi|^{-1} (d\varphi^*)^{-1} \eta(f) \delta_{\varphi(c(f))}, \quad (7)$$

where $d\varphi$ is the Jacobian matrix of φ and $|d\varphi|$ its determinant, evaluated at $c(f)$.

4 Diffeomorphic metric mapping

Having defined metrics between two unlabeled point sets and surfaces for completeness we briefly review metric on the space of Diffeomorphic transformations. To generate dense deformation maps in \mathbb{R}^d we use the large deformation framework [8] which consist of integrating time-dependent velocity fields in \mathbb{R}^d . The corresponding flow equation is given by

$$\frac{\partial \varphi^v(t, x)}{\partial t} = v(t, \varphi^v(t, x)), \quad (8)$$

with $\varphi(0, x) = x$, and we define $\varphi(x) := \varphi^v(1, x)$, which is a one-to-one map in \mathbb{R}^d (diffeomorphism). To ensure regularity of these maps, an energy functional is defined on velocity fields:

$$\|v(t, \cdot)\|_V^2 = \int_{\mathbb{R}^d} \langle Lv(t, x), Lv(t, x) \rangle dx, \quad (9)$$

where L is a differential operator acting on vector fields. Minimality constraints on this energy are included in the matching variational problems. Moreover, this energy also defines a distance in the group of diffeomorphisms:

$$D^2(e, \varphi) = \inf_{v, \varphi^v(1, \cdot) = \varphi} \int_0^1 \|Lv(t)\|_V^2 dt. \quad (10)$$

As was noticed in [13, 9, 10], the practical use of such models is simplified, in the context of point-based matching methods, by the fact that optimal vector fields take the form:

$$v(t, x) = \sum_{p=1}^n G(x_p(t), x) \alpha_p(t), \quad (11)$$

where $x_p(t) = \varphi^v(t, x_p)$ are the trajectories of the control points x_p , $G(x, y)$ is the Green kernel of operator L^*L , and $\alpha_p(t) \in \mathbb{R}^d$ are unknown variables called momentum vectors. From 8 and 11, one derives the equations which link trajectories and momentum vectors:

$$\frac{dx_p}{dt}(t) = \sum_{p_1=1}^n G(x_{p_1}(t), x_p(t)) \alpha_{p_1}(t). \quad (12)$$

Hence computing momentum vectors from trajectories requires to solve T linear systems, where T is the number of time discretization steps, while computing trajectories from momentum vectors requires to solve a first order ODE, which can be performed at a lower cost. Therefore, the choice of momentum vectors as variables of minimization is preferred in practice. The reformulation of the energy functional in terms of $x_p(t)$ and $\alpha_p(t)$ becomes:

$$\|v(t, \cdot)\|_V^2 = \sum_{p=1}^n \left\langle \frac{dx_p}{dt}(t), \alpha_p(t) \right\rangle. \quad (13)$$

5 Atlas construction for points sets and surfaces

Having defined the metrics on unlabeled point sets, surfaces and diffeomorphic transformations we are ready to apply the recipe of minimum mean squared estimation to the atlas construction problem.

5.1 Formulation for point sets

Let $\{x_{ip}\}$, $1 \leq i \leq N$, $1 \leq p \leq n_i$ be N unlabeled point sets in \mathbb{R}^d , and $a_{ip} \in \mathbb{R}$ the associated weights (e.g. $a_{ip} = \frac{1}{n_i}$). Let $\mu_i = \sum_{p=1}^{n_i} a_{ip} \delta_{x_{ip}}$ be the borel measure representation of each of the point sets. The template estimation is now defined as the following minimum mean squared estimation problem:

$$\{\hat{\varphi}_i, \hat{\mu}\} = \arg \min_{\varphi_i, \mu} \sum_{i=1}^N \left\{ \left\| \mu - \varphi_i \mu_i \right\|_K^2 + D^2(e, \varphi_i) \right\}, \quad (14)$$

where $D(e, \varphi_i)$ is the metric on the space of diffeomorphic mappings φ_i , described in section 4. This problem is simplified by the following remark: for fixed φ_i , the Borel measure $\hat{\mu}$ which minimizes 14 is the average of $\varphi_i \mu_i$:

$$\hat{\mu} = \frac{1}{N} \sum_{i=1}^N \varphi_i \mu_i = \frac{1}{N} \sum_{i=1}^N \sum_{p=1}^{n_i} a_{ip} \delta_{\varphi_i(x_{ip})}. \quad (15)$$

It is a sum of Dirac masses associated to the union of all points $\varphi_i(x_{ip})$. Consequently, minimization of 14 can be done with respect to deformation maps $\varphi_i(t)$ only:

$$\{\hat{\varphi}_i\} = \arg \min_{\varphi_i} \sum_{i=1}^N \left\{ \left\| \left(\frac{1}{N} \sum_{i=1}^N \varphi_i \mu_i \right) - \varphi_i \mu_i \right\|_K^2 + D^2(e, \varphi_i) \right\}. \quad (16)$$

5.2 Formulation for surfaces

Let S_i be N surfaces in \mathbb{R}^3 . Let $[S_i]$ denote either the current corresponding to S_i , or its approximation by a finite sum of vectorial Diracs. Note again that this sum is itself a current, and therefore the following is well defined for the continuous problem or its discretization. Using the metric defined on currents and diffeomorphic mappings in sections 2 and 4, the minimum mean squared error template estimation problem can now be formulated as:

$$\{\hat{\varphi}_i, [\hat{S}]\} = \arg \min_{\varphi_i, [S]} \sum_{i=1}^N \left\{ \left\| [S] - \varphi_i [S_i] \right\|_K^2 + D^2(e, \varphi_i) \right\}. \quad (17)$$

For fixed φ_i , the minimizer $[S]$ of 17 is the average of $\varphi_i [S_i]$: $[\hat{S}] = \frac{1}{N} \sum_{i=1}^N \varphi_i [S_i]$. This average $[S]$ is a current corresponding not to a single surface, but to the

union of the deformed surfaces $\varphi_i(S_i)$, each weighted by $\frac{1}{N}$. One can think about this as a sort of fuzzy surface and the exact interpretation of this is beyond the scope of this paper. However since it is a well defined current, the registration process of all the surfaces to the average current is well defined. The reformulation of 17, in terms of minimization with respect to the diffeomorphisms φ_i only, becomes:

$$\{\hat{\varphi}_i\} = \arg \min_{\varphi_i} \sum_{i=1}^N \left\{ \left\| \left(\frac{1}{N} \sum_{i=1}^N \varphi_i[S_i] \right) - \varphi_i[S_i] \right\|_K^2 + D^2(e, \varphi_i) \right\}. \quad (18)$$

6 Implementation

We now describe in detail an implementation for performing minimizations of 16 and 18 using an alternating algorithm which estimates, on a per iteration basis, each φ_i in turn, analogous to the method described in [2] for images. At each step, minimization is performed with respect to φ_i alone, the other deformation maps φ_j , $j \neq i$, being fixed, which transforms the whole averaging process into a sequence of source-to-target matchings, for which the algorithms described in [9] and [10] can be directly applied. More precisely, at each step of this sequence of matchings, we perform minimization of a functional involving an energy term and an end-point matching term:

$$J \left(\{\alpha_{ip}(t)\}_{1 \leq p \leq n_i}^{t \in [0,1]} \right) = \int_0^1 \sum_{p=1}^{n_i} \left\langle \frac{dx_{ip}}{dt}(t), \alpha_{ip}(t) \right\rangle dt + A(\{x_{ip}(1)\}). \quad (19)$$

Assuming that G is a function of the squared distance: $G(x, y) = G(|x - y|^2)$, the gradient becomes

$$\nabla J_{ip}(t) = 2\alpha_{ip}(t) + \beta_{ip}(t), \quad (20)$$

where $\beta_{ip}(t)$ is solution to the following ODE:

$$\begin{aligned} \frac{d\beta_{ip}}{dt}(t) = & -2 \sum_{p_1=1}^n G'(|x_{ip_1}(t) - x_{ip}(t)|^2) \left\{ \langle \alpha_{ip}(t), \beta_{ip_1}(t) \rangle + \right. \\ & \left. \langle \alpha_{ip_1}(t), \beta_{ip}(t) \rangle + 2 \langle \alpha_{ip}(t), \alpha_{ip_1}(t) \rangle \right\} (x_{ip}(t) - x_{ip_1}(t)), \end{aligned} \quad (21)$$

with $\beta_{ip}(1) = \nabla_{x_{ip}(1)} A$.

The matching term A , in the case of point sets, is given by:

$$\begin{aligned} A(\{x_{ip}(1)\}) = & \|\varphi_i \mu_i - \hat{\mu}\|_K^2 = \sum_{p=1}^{n_i} \sum_{p'=1}^{n_i} a_{ip} a_{ip'} K(x_{ip}(1), x_{ip'}(1)) \\ & - 2 \sum_{p=1}^{n_i} \sum_{q=1}^m a_{ip} b_q K(x_{ip}(1), y_q) + \sum_{q=1}^m \sum_{q'=1}^m b_q b_{q'} K(y_q, y_{q'}), \end{aligned} \quad (22)$$

where points y_q and weights b_q denote the average template $\hat{\mu}$ as follows:

$$\sum_{q=1}^m b_q \delta_{y_q} := \hat{\mu} = \frac{1}{N} \sum_{j=1}^N \sum_{p=1}^{n_j} a_{jp} \delta_{\varphi_j(x_{jp})}. \quad (23)$$

The gradient of this term, required for the computation of Eqn. 20, becomes:

$$\nabla_{x_{ip}(1)} A = 2a_{ip} \left(\sum_{p'=1}^n a_{ip'} \nabla_{x_{ip}(1)} K(x_{ip}(1), x_{ip'}(1)) - \sum_{q=1}^m b_q \nabla_{x_{ip}(1)} K(x_{ip}(1), y_q) \right). \quad (24)$$

We now follow the same recipe in the case of surfaces. Denote $\sum_{f_i=1}^{n_{f_i}} \eta(f_i) \delta_{c(f_i)}$ the sum of vectorial Diracs approximating each of the triangular meshes given by moving all vertices x_{ip} of S_i under the deformation map φ_i , and

$$\sum_{g=1}^m \eta(g) \delta_{c(g)} := \frac{1}{N} \sum_{i=1}^N \sum_{f_i=1}^{n_{f_i}} \eta(f_i) \delta_{c(f_i)} \quad (25)$$

the averaged template. The matching term becomes:

$$\begin{aligned} A(\{x_{ip}(1)\}) &= \sum_{f_i=1}^{n_{f_i}} \sum_{f'_i=1}^{n_{f_i}} \eta(f_i) * K(c(f_i), c(f'_i)) \eta(f'_i) \\ &- 2 \sum_{f_i=1}^{n_{f_i}} \sum_{g=1}^m \eta(f_i) * K(c(f_i), c(g)) \eta(g) + \sum_{g=1}^m \sum_{g'=1}^m \eta(g) * K(c(g), c(g')) \eta(g'). \end{aligned} \quad (26)$$

We recall that $x_{ip}(1) = \varphi_i(x_{ip})$ where x_{ip} are the vertices of the triangular mesh S_i . Centers and normal vectors are computed from the vertices using formulas in Eqn. 6. Finally, we derive the gradient of term A in this case. If $x_{ip}(1)$ is a vertex of face f_i , the contribution of f_i to the gradient at $x_{ip}(1)$ is given by

$$\begin{aligned} &\sum_{f'_i=1}^{n_i} e(f_i) \times K(c(f'_i), c(f_i)) \eta(f'_i) - \sum_{g=1}^m e(f_i) \times K(c(g), c(f_i)) \eta(g) \\ &+ \frac{2}{3} \sum_{f'_i=1}^{n_i} \frac{\partial K(c(f_i), c(f'_i))}{\partial c(f_i)} \eta(f'_i) - \frac{2}{3} \sum_{g=1}^m \frac{\partial K(c(f_i), c(g))}{\partial c(f_i)} \eta(g), \end{aligned} \quad (27)$$

and gradient $\nabla_{x_{ip}(1)} A$ is obtained by summing all contributions of faces f_i which share $x_{ip}(1)$ as a vertex.

Having computed the gradients, a conjugate gradient method is used to perform minimization of functional J on variables $\alpha_p(t)$ evaluated on finite number

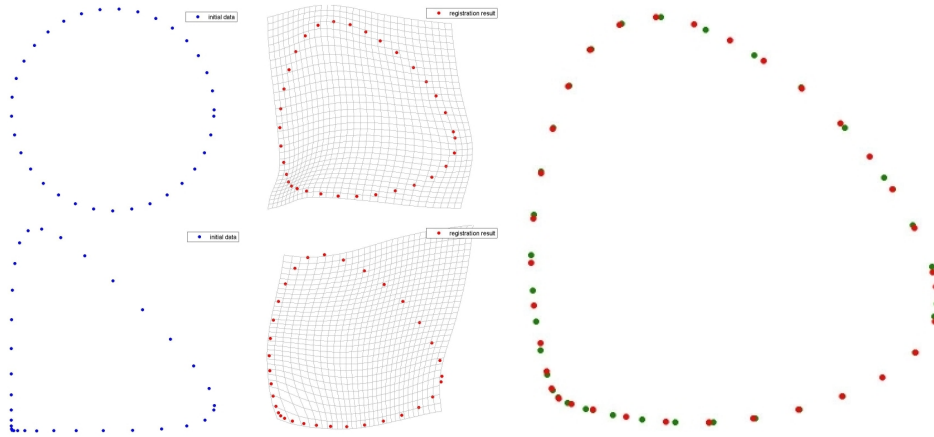


Fig. 1. Experiment with synthetic 2d data. Left column: the two unlabeled point sets; middle: deformed point sets and deformation of a grid; right: averaged template, composed of the two deformed point sets.

of time steps regularly spaced between 0 and 1, and a centered corrector scheme is applied to solve ODE 21, required for each computation of gradient 20. To speed up computations when a large number of control points is involved, we use multipole[?] methods for convolutions with kernels G and K .

7 Results

We now present results from applying the algorithms described previously. Figure 1 shows a synthetic experiment of averaging two point sets in \mathbb{R}^2 , which are drawn from a circle and another oblong closed curve (shown in the left column). Shown in the middle column are the results of applying the estimated deformation to the two data sets. Shown in the right column is the average estimated template.

Figure 2 shows an example of averaging three segmented surfaces of hippocampus in \mathbb{R}^3 . Shown in the top row are three surfaces of hippocampi from three different subjects. The middle row shows the estimated deformation applied to each of the surfaces. Shown at the bottom is the estimated template.

8 Discussion

References

1. Joshi, S., Davis, B., Jomier, M., Gerig, G.: Unbiased diffeomorphic atlas construction for computational anatomy. *NeuroImage* **23** (2004) s151–s160

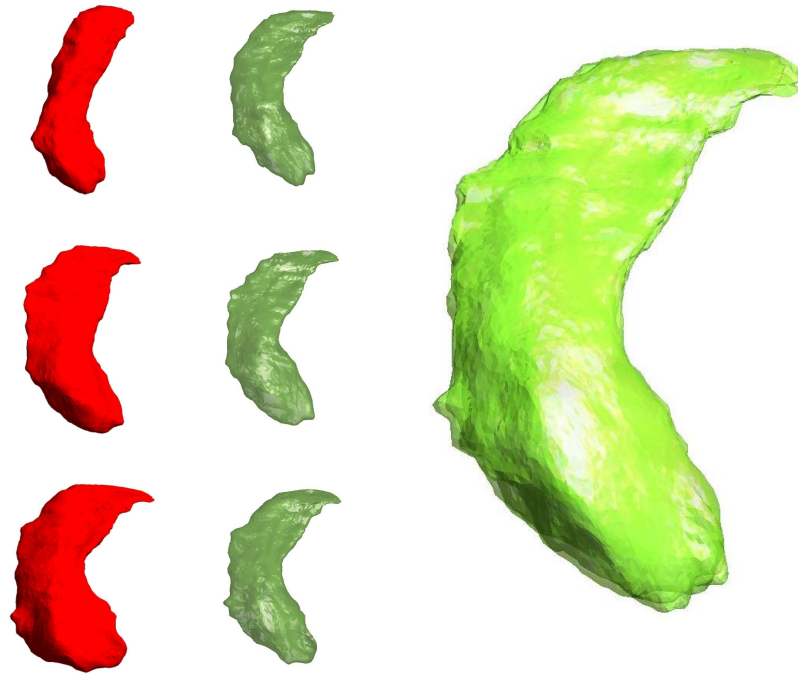


Fig. 2. Experiment with hippocampus surface data. Top row shows the three segmented surfaces of hippocampus, middle row shows the three deformations of the surfaces, and bottom is the averaged template which is composed by these three deformed surfaces.

2. P. Lorenzen, B. Davis, S.J.: Unbiased atlas formation via large deformations metric mapping. In: MICCAI. (2005)
3. Grenander, U., Miller, M.I.: Computational anatomy: An emerging discipline. Quarterly of Applied Mathematics **56** (1998) 617–694
4. Grenander, U.: General Pattern Theory. Oxford Univ. Press (1994)
5. Joshi, S., Grenander, U., Miller, M.: On the geometry and shape of brain sub-manifolds. International Journal of Pattern Recognition and Artificial Intelligence: Special Issue on Processing of MR Images of the Human **11** (1997) 1317–1343
6. Frechet, M.: Les elements aleatoires de nature quelconque dans un espace distance. Annales De L’Institut Henri Poincare **10** (1948) 215–310
7. Trouvé, A., Younes, L.: Metamorphoses through lie group action. Foundations of Computational Mathematics **5** (2005) 173–198
8. Miller, M, I., Younes, L.: Group action, diffeomorphism and matching: a general framework. Int. J. Comp. Vis **41** (2001) 61–84 (*Originally published in electronic form in: Proceeding of SCTV 99, <http://www.cis.ohio-state.edu/szhu/SCTV99.html>*).
9. Glaunès, J., Trouvé, A., Younes, L.: Diffeomorphic matching of distributions: A new approach for unlabelled point-sets and sub-manifolds matching. In: CVPR, IEEE Computer Society (2004) 712–718

10. Vaillant, M., Glaunes, J.: Surface matching via currents. In Christensen, G.E., Sonka, M., eds.: IPMI. Volume 3565 of Lecture Notes in Computer Science., Springer (2005) 381–392
11. Federer, H.: Geometric measure theory. Springer-Verlag (1987)
12. Morgan, F.: Geometric measure theory, 2nd ed. Acad. Press, INC. (1995)
13. Joshi, S., Miller, M.: Landmark matching via large deformation diffeomorphisms. IEEE transactions in image processing **9** (2000) 1357–1370